Journal of Applied Polymer Science

Design of renewable poly(amidoamine)/hemicellulose hydrogels for heavy metal adsorption

Elena Ferrari,[1] Elisabetta Ranucci,[1] Ulrica Edlund,[2] Ann-Christine Albertsson[2]
[1]Dipartimento di Chimica, University of Milan, 20133 Milano, Italy
[2]Fibre and Polymer Technology, Royal Institute of Technology (KTH), Teknikringen 56–58, SE-100 44, Stockholm, Sweden
Correspondence to: A.-C. Albertsson (E-mail: aila@kth.se)

ABSTRACT: Renewable poly(amidoamine)/hemicellulose hydrogels were prepared from *O*-acetylated galactoglucomannan (AcGGM)-rich biomass and shown to display a significantly high adsorption capacity for Cu^{2+}, Cd^{2+}, $Pb^{2+,}$ Zn^{2+}, Ni^{2+}, Co^{2+}, and CrO_4^{2-}. Two different acrylamido end-capped poly(amidoamine) oligomers (PAA) were prepared and covalently immobilized onto an *in situ* formed polysaccharide network via water-based free radical graft copolymerization and cross-linking. The synthetic approach was shown to be viable when using a highly purified AcGGM or a crude spruce hydrolysate, an AcGGM and lignin containing biomass fraction as a reactant. Homogeneous reaction mixtures were obtained in both cases with polysaccharide contents up to 20% by weight. Oscillatory shear measurements indicated a predominantly solid-like behavior of the hydrogels with an increase in shear storage modulus with increasing cross-link density. The mechanical integrity of the PAA/hemicellulose hydrogels showed higher water swelling capacity and less fragility than the parent PAA hydrogels and they retained the heavy metal ion absorption ability of the PAA component, even in the presence of the least purified hemicellulose fraction.
 J. Appl. Polym. Sci. **2015**, *132*, 41695.

KEYWORDS: addition polymerization; biopolymers and renewable polymers; gels; polysaccharides; properties and characterization

Received 12 September 2014; accepted 31 October 2014
DOI: 10.1002/app.41695

INTRODUCTION

Bioadsorption of heavy metal ions by functional hydrogels is emerging as a promising alternative to conventional methods in the treatment of waste waters. Water contamination by heavy metal ions derived from industrial and manufacturing practices, mainly metal working operations and textile factories, represents a global environmental problem. These substances elicit severe ecological and health effects even at trace levels due to their strong toxicity, persistence, and tendency to bioaccumulate.[1,2] As three-dimensional hydrophilic networks, hydrogels offer many advantages in the removal of water contaminants, offering very high water absorption and retention capacities and high permeability to small molecules. Even more attractive is the potential production of functional hydrogels from renewable resources (natural resources that are regenerated within the time frame for its consumption), aiming to produce materials with a more sustainable track record and potential biodegradability. Polysaccharides stand out as potent macromolecular candidates for renewable hydrogel design because they are abundant in nature, nontoxic, easily extracted from bio-based feedstock and inherently hydrophilic. The swelling of polysaccharides in water and their adsorption of aqueous solutes can be controlled via their cross-linking density and chemistry. Among the many polysaccharide-based hydrogels described in the literature, a few have been specially prepared for heavy metal adsorption. Pectin cross-linked with glycidyl methacrylate was shown to have a high adsorption capacity for Cu^{2+} and Pb^{2+} from a slightly acidic aqueous solution.[3] Chitosan contains numerous amine pendant groups that may act as chelating groups. A chitosan-derived hydrogel was shown to be effective for Cu^{2+} adsorption,[4] whereas an amino-functionalized dextran hydrogel showed a particular affinity for Zn^{2+}.[5] Furthermore, a salep sulfate-graft-polyacrylic acid hydrogel was demonstrated to remove Co^{2+}, Zn^{2+}, and Cu^{2+} from an aqueous solution.[6]

Hemicelluloses, amorphous polysaccharides located in the secondary cell wall of woods and grasses, are abundantly available renewable resources and can be obtained through a range of lignocellulosic biorefining processes. Xylans and mannans are the major types of hemicelluloses that occur in wood, and the material and chemical utilization of this biomass does not compete with food production. The poly-hydroxylated structure of these hemicelluloses renders them strongly hydrophilic and

Additional Supporting Information may be found in the online version of this article.

open to chemical modification, hence making them potent candidates for functional hydrogel production. *O*-acetyl-galactoglucomannan (AcGGM) in softwood has a nonlinear acetylated structure and is typically completely water-soluble, facilitating chemical functionalization, and integration into green chemistry procedures in the design of value-added products such as films,[7–9] bio-based fuels,[10,11] and hydrogels.[12–15] A xylan hydrogel designed to adsorb heavy metals was prepared by copolymerization with acrylic acid and shown to efficiently adsorb Cd^{2+}, Pb^{2+}, and Zn^{2+} from aqueous solution.[16] Similarly, but to a lesser extent, a hydrogel prepared from arabinoxylan and acrylic acid adsorbed Cu^{2+} and Ni^{2+}.[17] AcGGM functionalized and cross-linked with glycidyl methacrylate and [2-(methacryloyloxy)ethyl]trimethylammonium chloride was prepared for the adsorption of Cr^{6+} and As^{5+}.[18]

The fractionation and purification of hemicelluloses from lignocellulosic feedstock is typically a tedious and costly process. From a sustainability and economic perspective, less-refined hemicellulose biomass would be more viable as macromer fractions in renewable hydrogel design. Wood hydrolysates represent this type of biomass, containing hemicelluloses as a major component and a smaller yet significant amount of lignin and being produced world-wide on a large scale in industrial wood processing operations such as pulping. Biorefining initiatives to utilize noncellulosic wood polysaccharides are thus preferably accompanied by the parallel development of synthetic pathways that are robust to the presence of lignin and water in hydrolysate fractions.[19,20]

Selective functionalization of polysaccharide structures, whether highly purified or crude, in conjunction with vinyl polymerization offers a range of new opportunities to derive hydrogels with innovative combinations of chemical and physical properties. The radical graft copolymerization of vinyl monomers onto polysaccharide backbones is mediated by the presence of radical initiators that generate alkoxy radicals capable of initiating propagating chain growth of the vinyl monomer from the polyhydroxylated polysaccharide chain. In the presence of suitable cross-linking agents, polysaccharide hydrogels are obtained. If a polysaccharide such as AcGGM is reacted with a functional component, thereby inducing a strong ability to complex heavy metal ions, functional, insoluble cross-linked bioadsorbing copolymers can be obtained. Poly(amidoamine)s (PAAs) represent promising functional additives and also provide an opportunity to prepare materials via greener chemistry. PAAs constitute a family of highly hydrophilic, biodegradable, and biocompatible synthetic polymers prepared in aqueous solution, at room temperature and with no added catalysts or organic solvents. A wide range of functional amines and bisacrylamides can be used as monomers for their syntheses. PAAs are endowed with the ability to yield complexes with many heavy metal ions.[21–24]

Our aim was to combine PAAs and AcGGM biomass in the design of heavy metal complexation hydrogels through a water-based pathway and assess their potential to perform, with adequate mechanical integrity, as efficient wastewater treatment gels, in particular adsorbing Cu^{2+}, Cd^{2+}, Pb^{2+}, Zn^{2+}, Ni^{2+}, and Co^{2+} from aqueous solutions. The hydrogel preparation pathway was robustly designed to allow for less refined hemicellulose-rich biomass to be used as a reactant while retaining product function.

EXPERIMENTAL

Materials

All chemicals, unless otherwise indicated, were used as received. *N,N*Ç-methylenebisacrylamide (MBA) (99%), NaOH (99%), $LiOH{\cdot}H_2O$ (99%), HCl (32%), 2-methylpiperazine (MP) (98%), glycine (Gly) (99%), methacrylic acid (99%), $Na_2S_2O_5$ (99%), $(NH_4)_2S_2O_8$ (99%), ethylenediaminetetraacetic acid disodium salt (EDTA-Na_2) (98.5%), Eriochrome® Black T (indicator grade), Murexide (for complexometry), NH_4Cl (≥99.5%), NH_4OH solution (28% NH_3 in H_2O, ≥99.9%), K_2CrO_4 (≥99%), Cu^{2+}, Ni^{2+}, Co^{2+}, and Pb^{2+} nitrate (99.99% on metal basis) were purchased from Sigma Aldrich. Cd^{2+} nitrate (99.99% on metal basis) was purchased from Alfa Aesar. Zn^{2+} sulfate heptahydrate was purchased from Kebo. *N,N*Ç-dimethylethylenediamine (DMEDA) (85%) was purchased from Acros.

Purified *O*-acetylated galactoglucomannan (AcGGM) was recovered from the aqueous fraction generated by thermomechanical pulping spruce (*Picea abies)* wood. The aqueous phase was fractionated and concentrated by ultrafiltration and freeze-dried (Lyolab 300 lyophilizer). The solid product contained <1% lignin and had a carbohydrate composition of 17% glucose, 65% mannose, 15% galactose, as determined by the method of Dahlman *et al.*[25] AcGGM had a number average molecular weight (M_n) of ∼7500 g mol^{-1} (DP ∼ 40), a dispersity (Đ) of 1.3 and a degree of acetylation (DS_{Ac}) of 0.3, as determined by size exclusion chromatography (SEC) calibrated with MALDI-TOF according to a published protocol.[26]

A spruce hydrolysate, an aqueous fraction containing mostly AcGGM but also 5% xylan and 15% lignin, was obtained in the hydrothermal treatment of wood chips as previously described.[27] The process liquor was subjected to ultrafiltration and freeze-dried (Lyolab 300 lyophilizer). The hydrolysate had a weight average molecular weight (M_w) of ∼2500 g mol^{-1} and a dispersity (Đ) of 3. The carbohydrate and lignin composition was determined as previously described[27] and is given in Table S1 in the Supporting Information.

Synthesis of Acrylamide End-Capped Poly(amidoamine) Oligomers (PAAs)

MBAMP Oligomers. MBA (7.76 g; 49.82 mmol) and MP (3.56 g; 34.87 mmol) were mixed in water (16.61 mL) and maintained at 40°C, in the dark, under stirring. The mixture, which became a clear solution after 12 h, was allowed to react for 72 h, then diluted with H_2O (150 mL) and freeze-dried. The final product was recovered as a white powder. Yield: 11.3 g, 99.8%. ^{1}H NMR (400 MHz, D_2O, 298 K): 6.14 (br, H1), 5.69 (br, H2), 4.62-4.44 (H4, H4'), 2.96-1.75 (br, -MP ring and -CH_2- polymer chain), 0.94 (br, H10). ^{13}C NMR (100 MHz, D_2O, 298 K): 175.19 (C15,C17), 168.61 (C3,C5), 129.50 (C2), 128.21 (C1), 58.61 (C8), 53.61 (C9), 52.90 (C11), 51.45 (C12), 49.76 (C13), 48.20 (C7), 44.24 (C4), 32.27 (C14), 30.76 (C6),

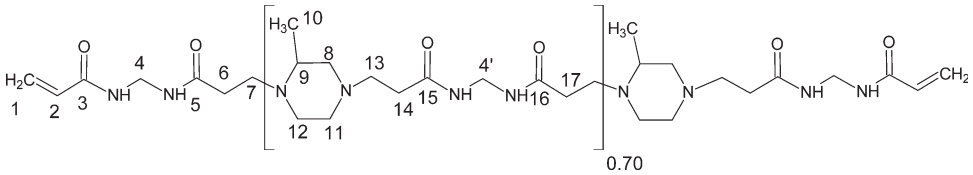

Figure 1. Atom labeling of MBAMP for NMR peak assignments.

15.84 (C10). SEC: $M_n = 4370$ g mol^{-1}, (Đ)=1.00. The NMR peak assignments are shown in Figure 1.

MBAGD Oligomers. MBAGD oligomer was prepared by adding MBA (7.76 g; 49.82 mmol) then Gly (1.32 g; 17.44 mmol) together with LiOH•H_2O (746.72 mg; 17.44 mmol) and finally DMEDA (2.21 mL; 17.44 mmol) to a H_2O:MeOH = 1 : 1 solution (16.61 mL) following the same procedure reported for MBAMP. The product was recovered as a light-yellow powder. Yield: 11.59, 99.2%. ^{1}H NMR (400 MHz, D_2O, 298 K): 6.14 (br, H1), 5.69 (br, H2), 4.62-4.45 (H4, H4' and H4"), 3.02 (s, H18), 2.73-2.30 (br, -CH_2- polymer chain), 2.17 (s, H8, H8'). ^{13}C NMR (100 MHz, D_2O, 298 K): 178.76 (C19), 175.18 (C5, C3), 168.55 (C12, C12', C17), 129.56 (C2), 128.22 (C1), 57.41 (C7, C10), 53.00 (C9, C9'), 52.43 (C14, C15), 49.33 (C18), 44.35 (C4, C4', C4"), 41.65 (C8, C8'), 32.94 (C13, C16), 32.51 (C11, C6). SEC: $M_n = 1760$ g mol^{-1}, (Đ) = 1.08. The NMR peak assignments are shown in Figure 2.

Synthesis of Hydrogels

PAA-MA-AcGGM and PAA-MA-Hydrolysate. Hydrogels and the *in situ* grafting of PAA oligomers onto the AcGGM backbone were achieved by dissolving AcGGM (either purified or the hydrolysate) and LiOH•H_2O in H_2O in the dark under N_2(g). MA and then PAA (either MBAMP or MBADG) were added, and the polymerizations were then initiated by $Na_2S_2O_5$ and $(NH_4)_2S_2O_8$ (each 5 mg/μL aqueous solutions, 1% w/w). After 24 h of reaction at room temperature, each product hydrogel was removed from the reaction solution and soaked in 100 mL fresh deionized H_2O for 48 h, with the solvent renewed at regular time intervals. Finally, the hydrogels were dried until they had reached a constant weight. A series of hydrogels was prepared using this procedure by varying the reactants and amounts thereof as specified in Table I.

PAA-MBA-AcGGM. A hydrogel was prepared using an alternative procedure in which AcGGM (150.9 mg, 078 hexose mmol) and NaOH (102.7 mg, 2.51 mmol) were dissolved in 2.5 mL H_2O at 40°C for 20 min. MBA (194.5 mg, 1.25 mmol) was then added under stirring, and the mixture was allowed to react at 25°C for 20 h. The hydrogel was then removed from the reaction vessel and washed with 200 mL deionized H_2O for 48 h, with the solvent renewed at regular time intervals. Finally, the hydrogel was dried until it had reached a constant weight. The AcGGM content of the final hydrogel was 43.7% and the reaction yield 57.1%. This hydrogel is herein denoted MBA-A.

Characterization

NMR. ^{1}H and ^{13}CNMR spectra of PAA oligomers were obtained using a Bruker Avance DPX-400 NMR operating, respectively, at 400.13 MHz and 100.40 MHz. D_2O (Larodan Fine Chemicals AB) was used as a solvent, and spectra were recorded in sample tubes with an outer diameter of 5 mm. MestReNova software was used for data acquisition.

Molecular Weight. PAA oligomers' size exclusion chromatography (SEC) traces were obtained with Toso-Haas TSK-gel G4000 PW and TSK-gel G3000 PW columns connected in series using a Waters model 515 HPLC pump equipped with a Knauer autosampler 3800, a light scattering and viscometer Viscotek 270 dual detector, a UV detector Waters model 486 operating at 230 nm and a refractive index detector (Waters, Model 2410). The mobile phase was 0.1*M* Tris buffer (pH 8.00 ± 0.05) mixed with 0.2*M* sodium chloride. The flow rate was 1 mL min^{-1}, and the sample concentration was 1% (w/w).

FTIR. The hydrogels were dried under vacuum to constant weight, and FTIR spectra were collected using a Perkin Elmer spectrometer 2000 with an attenuated total reflectance (ATR) crystal accessory (Golden Gate). Each spectrum was calculated as the mean of 16 individual scans at a resolution of 2 cm^{-1} over the range of 4000–600 cm^{-1}, with corrections made for atmospheric water and carbon dioxide.

Hydrogel Swelling. The swelling degrees (SD) were evaluated in deionized H_2O, in 0.01*M* PBS at pH 7.4, in KCl/HCl buffer at pH 2 and in TRIS/HCl buffer at pH 9 at 20°C. The degree of swelling was determined by the following equation:

$$SD[\%] = \frac{m_{eq}}{m_0} \times 100$$

where m_{eq} is the weight of the sample at equilibrium and m_0 the weight of the dry sample.

Thermal Analyses

DSC analyses were performed on a Mettler Toledo DSC823e using 10 mg samples under nitrogen flow at 20 mL min^{-1} and a heating/cooling rate of 30°C min^{-1}. A first heating cycle from 0°C to 100°C was followed by a cooling cycle from 100°C to 0°C and a second heating cycle from 0 to 400°C. TGA analyses

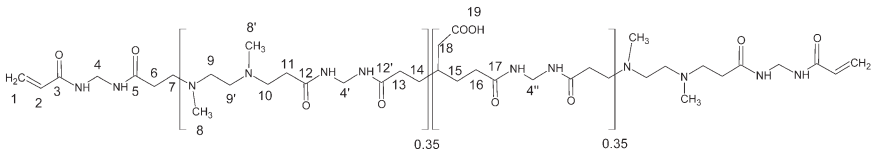

Figure 2. Atom labeling of MBAGD for NMR peak assignments.

Table I. Reagents and Amounts Used in the Syntheses of PAA-MA-Hemicellulose Hydrogels.

Sample	PAA type	Hexose units/MA/PAA acrylamide terminals (molar ratio)	Hemi-cellulose type	Hemi-cellulose content[a] (%)	$LiOH•H_2O$ amount (mmol)	H_2O mL	MA content[a] (%)	PAA content[a] (%)
MBAMP-0	MBAMP	0/0/1	AcGGM	0.0	1.4	1.5	0.0	100
MBAMP-A	MBAMP	1.04/0.24/1	AcGGM	20.6	1.4	2	2.1	77.3
MBAMP-H	MBAMP	0.48/1.26/1	Hydrolysate	11.3	2.17	1.5	11.3	77.4
MBAGD-0	MBAGD	0/0/1	AcGGM	0.0	1.4	1.5	0.0	100
MBAGD-A	MBAGD	1/0.23/1	AcGGM	20.6	1.4	2	2.1	77.3
MBAGD-H	MBAGD	0.45/1.19/1	Hydrolysate	11.3	2.17	1.5	11.3	77.4

[a] In the feed.

were performed on a Perkin Elmer TGA 4000 using 10 mg samples under nitrogen flow at 50 mL min^{-1} from 30°C to 600°C at a heating rate of 30°C min^{-1}.

Dynamic Mechanical Analyses

Rheological characterizations were performed on a TA instrument model AR2000. Samples obtained via route 1 were prepared as discs with a thickness of 2 mm and a base diameter of 0.8 cm. Samples obtained via route 2 were prepared as discs with a thickness of 5 mm and a base diameter of 2.5 cm. All samples were allowed to swell to equilibrium for 72 h. Sweep tests (strain-controlled) were performed at 25°C with samples held at 0.2% strain over a frequency range of 0.5 to 100 rad s^{-1}. A parallel plate geometry was used.

Heavy Metal Ion Absorption. Metal ions absorption tests were carried out against Cu^{2+}, Co^{2+}, Pb^{2+}, Cd^{2+}, Zn^{2+}, Ni^{2+}, and CrO_4^{2-}. Standardized aqueous solutions at 700 ppm were employed for all of the heavy metals. Pb^{2+} and Cd^{2+} absorption was also tested by starting from 50 ppm solutions, and

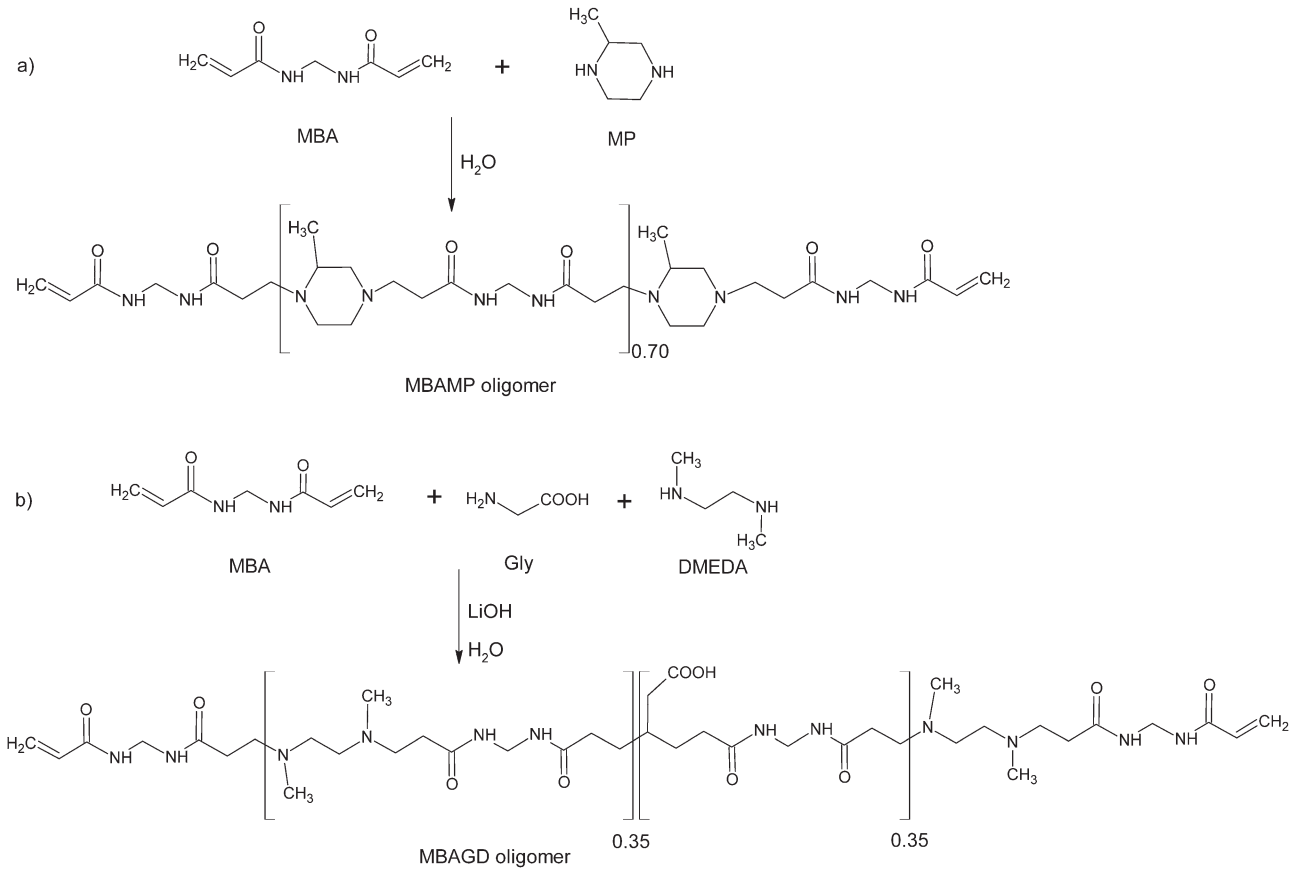

Scheme 1. Syntheses of acrylamide-end-capped PAA oligomers.

Table II. Results of the Elemental Analysis for AcGGM- and PAA-Based Hydrogels

	C %		N %		C/N		PAA[a] %(w/w)	
Sample	calc.[a]	Found	calc.[a]	Found	calc.[a]	Found	Feed[a]	Found[b]
AcGGM	48.8	-	-	-	-	-	-	-
MBA-A	51.8	42.4	10.6	7.8	4.9	5.4	56.3[c]	43.1[c]
MBAMP-0	56.1	50.6	21.2	19.7	2.7	2.6	100	96.6
MBAMP-A	50.4	48.5	15.6	16.0	3.2	3.0	77.3	81
MBAMP-H	50.5	46.5	15.3	15.0	3.3	3.1	77.4	76
MBAGD-0	51.6	47.9	20.2	21.2	2.6	2.3	100	88.3
MBAGD-A	48.2	46.0	16.7	16.5	2.9	2.8	77.3	78
MBAGD-H	48.2	44.4	16.4	15.2	2.9	2.9	77.4	71.8

[a] Feeding data from Tables I and II.
[b] Calculated values.
[c] MBA content.

CrO_4^{2-} adsorption was tested by starting from 4 ppm solutions. The absorption tests were performed by using 10 mg of dried hydrogel in a 10 mL tube and swelling it to equilibrium in deionized water (10 mL) for 24 h. The supernatant was then replaced with a heavy metal aqueous solution, and the hydrogel was incubated in this solution for another 12 h. The initial and the final supernatant metal concentrations were determined via complexometric titration with EDTA for all of the metals, whereas CrO_4^{2-} was measured photometrically after lowering the pH of the solution to 2 with HCl ($\lambda_{max} = 350.9$ nm).[28]

EDTA-Na_2 standardization: A1 $\times$ 10^{-4} M $ZnSO_4 \cdot 7H_2O$ solution was prepared, added to NH_4Cl/NH_3 buffer (pH $\sim$ 10) until an alkaline pH level was reached and titrated with a 1 $\times$ $10^{-4}M$ EDTA-Na_2 solution using Eriochrome® Black T as an indicator. The aqueous solution concentrations of Cd^{2+}, Pb^{2+}, and Zn^{2+} were determined by adding NH_4Cl/NH_3 buffer until an alkaline pH was reached in the presence of Eriochrome® Black T as an indicator and by titrating with the standardized EDTA-Na_2 solution. Ni^{2+}, Co^{2+}, and Cu^{2+} were titrated according to the same procedure described for Cd^{2+}, Pb^{2+}, and Zn^{2+}, employing Murexide as an indicator.

RESULTS AND DISCUSSION

Hemicelluloses, with their polyhydroxylated backbone, are potent renewable macromers for the preparation of hydrogels; indeed, the properties of hemicelluloses may be varied over wide ranges. The hemicellulose AcGGM is released to the aqueous phase in softwood pulping industries and thus is a potentially highly valuable macromer product derived from wood biorefineries. AcGGM, which also occurs in a less purified state, was here utilized as a matrix component in heavy-metal-adsorbing hydrogel matrices. A robust and green pathway was developed for the preparation of these matrices.

Hydrogel Synthesis

The hydrogel synthetic pathway consisted of two steps. First, two different acrylamide-end-capped PAA oligomers were prepared by employing a controlled excess of acrylamide, freeze-dried and recovered as fine powders. As shown in Scheme 1, the PAA oligomers were synthesized by a polyaddition of *N,N*'-methylenebisacrylamide with (a) 2-methylpiperazine (MBAMP) or (b) a mixture of glycine and *N,N*'-dimethylethylenediamine as amine counterparts (MBAGD). MBAMP and MBAGD represent models of cost-effective cationic or amphoteric PAAs. The structures of the products were verified by ^{1}H- and ^{13}CNMR, and the corresponding spectra are shown in the Supporting Information (Figure S1).

In the second step, MA was grafted onto either AcGGM or spruce hydrolysate in water using the metabisulfite/ammonium peroxydisulfate redox system as initiator and cross-linked *in situ* with either MBAMP or MBAGD. MA was chosen based on its controllable reactivity and importance as a monomer widely used for the preparation of hydrogels. MA-based hydrogels find numerous applications in various fields, from therapeutics to environmental applications.[29–32] The proposed mechanism for the copolymerization of MA in the presence of AcGGM and PAA oligomers is shown in Scheme 2. Partial deacetylation of the AcGGM will occur during synthesis given the alkaline conditions. It is known that, for many polysaccharides, the radicals resulting from the radical initiator generate active centers on the substrate, which extract hydrogens from hydroxyl groups to form alkoxy radicals.[33] These active centers initiate the radical polymerization of MA, thus producing a covalently linked hydrogel when a cross-linking agent is present in the system, e.g., MBAMP or MBAGD. In this system, the redox couple may, to some extent, also initiate MA homopolymerization that does not contribute to the cross-linking density of the network. To ensure complete removal of any such homopolymers, the crude hydrogels were soaked in fresh water until they had reached a constant weight. Following the elaborated synthetic pathway, two PAA-MA-AcGGM (samples MBAMP-A and MBAGD-A) and two PAA-MA-hydrolysate (samples MBAMP-H and MBAGD-H) hydrogels were obtained. Their behavior was compared with that of the corresponding "homopolymeric" PAA hydrogels prepared under identical conditions but in the absence of MA and AcGGM (MBAMP-0 and MBAGD-0, respectively). To allow for further comparisons, a hydrogel without MA and PAA, herein denoted MBA-A, was prepared by reacting AcGGM with MBA in a basic aqueous solution.

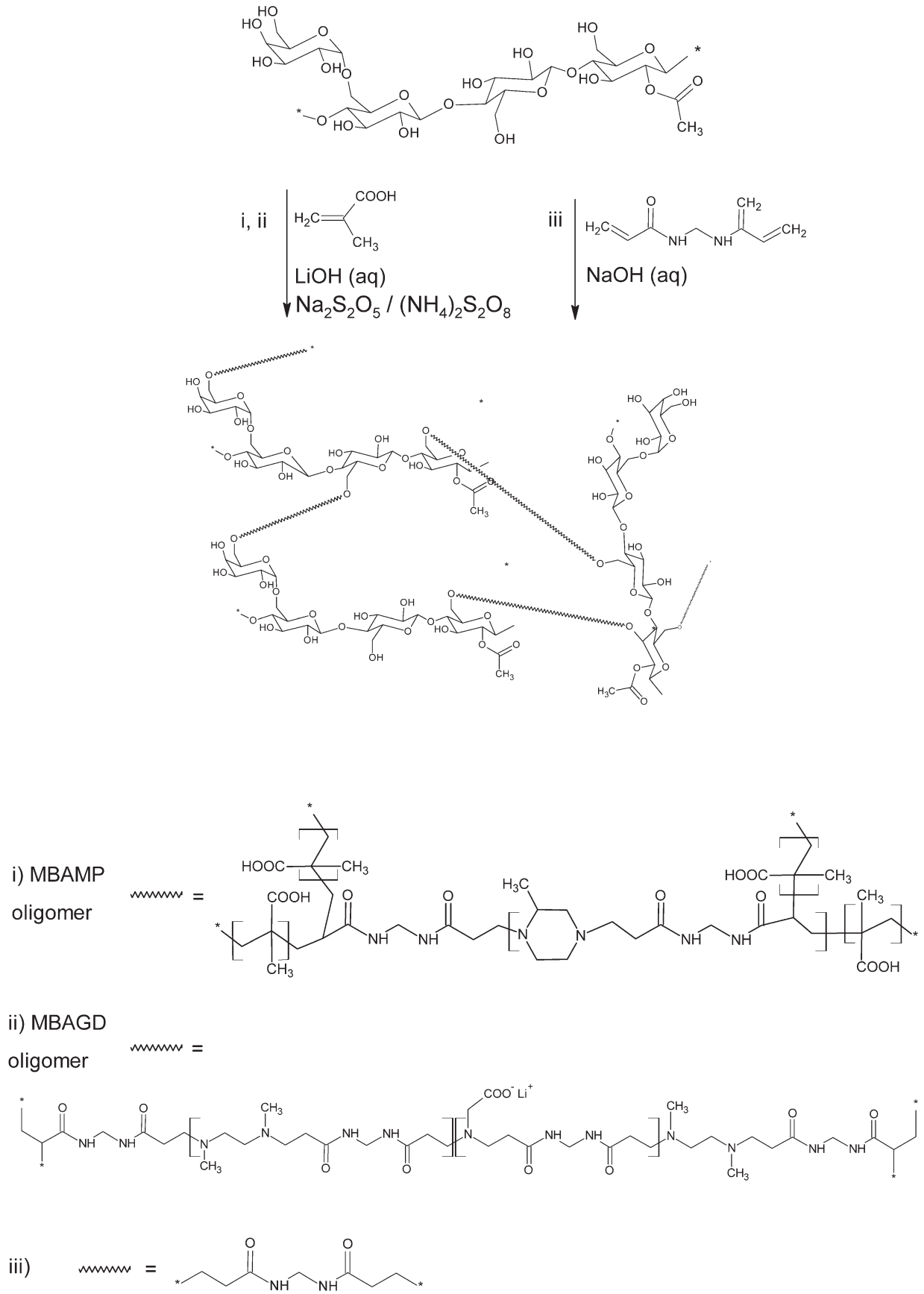

Scheme 2. Schematic syntheses of hemicellulose hydrogels using end-capped PAA oligomers or MBA as cross-linkers in aqueous basic media.

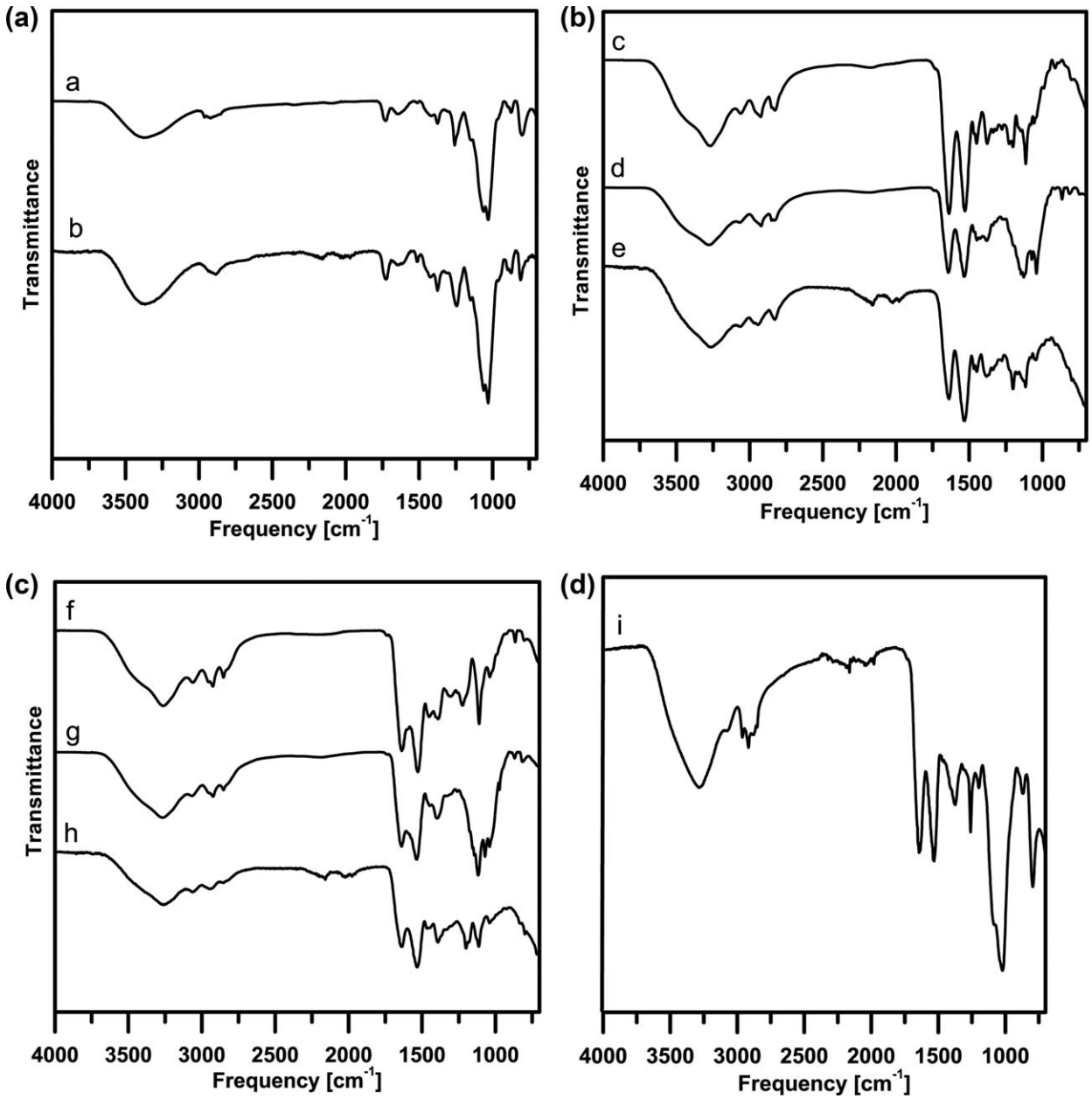

Figure 3. FTIR spectra of AcGGM-, spruce hydrolysate-, and PAA-based hydrogels: (a) AcGGM, (b) spruce hydrolysate, (c) MBAMP-0, (d) MBAMP-A, (e) MBAMP-H, (f) MBAGD-0, (g) MBAGD-A, (h) MBAGD-H, and (i) MBA-A.

Because of the solubility limit of the spruce hydrolysate fraction, its feed amount in synthesis was equal to 11.3% (w/w), whereas the amount of AcGGM in the feed was kept higher: 20.6% (w/w) (Table I). The PAA content in the feeding was ~77% (w/w) regardless of the type of PAA, and the overall concentration of solids was 25% (see Experimental). Polymerization experiments were also initially carried out with either PAA/AcGGM or PAA/MA mixtures but resulted in poor products. The former produced viscous, seemingly uncross-linked mixtures, which clearly indicated degradation over prolonged reaction times. The latter turned into hard and apparently highly cross-linked solids with low, if any, water swelling ability. For this reason, the use of mixtures containing all three components (PAA, MA, and either AcGGM or hydrolysate) was necessary to obtain covalently cross-linked and coherent hydrogels retaining their integrity in the swollen state. The hydrolysate contains a small fraction of lignin in addition to the main component AcGGM. Yet, the synthesis was not controlled in any way to ensure that only AcGGM reacted. As shown in previous work, the presence of lignin in the hydrolysate does not significantly interfere with radically initiated modification of AcGGM other that lowering the yield somewhat.[20]

All hydrogel samples were analyzed by elemental analysis to verify the composition (Table II). The C/N ratios of the hemicellulose-based gels were consistently higher than those

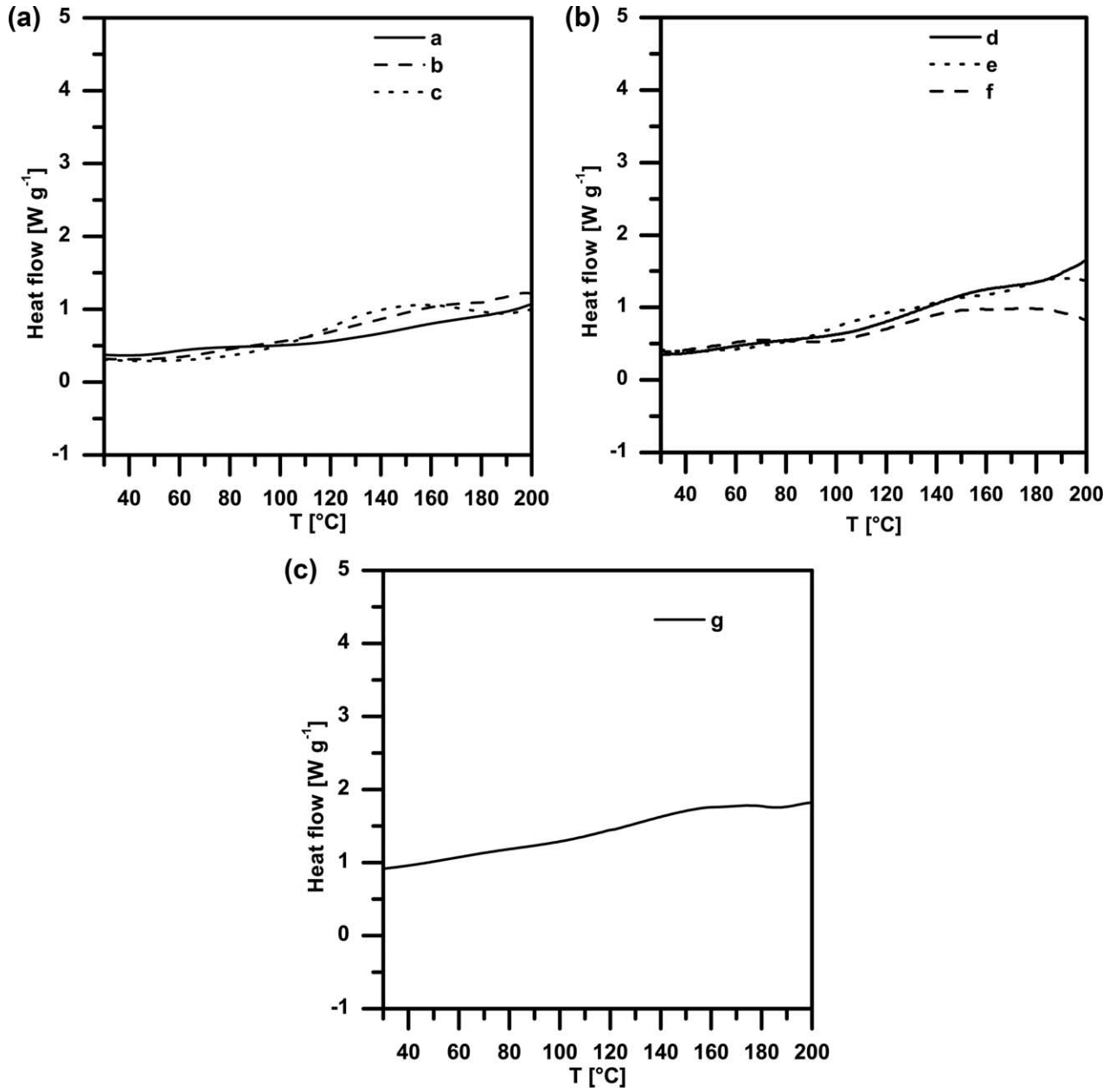

Figure 4. DSC thermograms for second heating cycle of PAA-based hydrogels: (a) MBAMP-0, (b) MBAMP-A, (c) MBAMP-H, (d) MBAGD-0, (e) MBAGD-A, (f) MBAGD-H, and (g) MBA-A.

of the reference homopolymeric PAA hydrogels (MBAMP-0 and MBAGD-0), indicating the presence of polyMA and AcGGM in the hydrogel structure. The C/N ratios were in all cases slightly lower than those theoretically expected, indicating a preferential release of noncross-linked AcGGM and homopolymerized MA during the post-polymerization washing process. The *N*% values allowed for the calculation of the PAA content in the hydrogels and a comparison with feed data (Table II).

FTIR spectrophotometry further revealed the structural composition of the prepared hydrogels (Figure 3). The spectra of PAA containing hydrogels all showed intense diagnostic bands typical of the PAA pattern, such as the amide C═O stretching band (1642 cm^{-1} for MBAMP-A, 1637 cm^{-1} for MBAGD-A), N—H bending and C—N stretching 1529 cm^{-1} bands overlapped with the carboxylate C═O symmetric stretching band of the MA repeating units, which prevailed over the remaining portion of the spectra. An asymmetric –COO- stretching band was also observed at 1446 cm^{-1} for MBAMP-A and MBAMP-H and 1454 cm^{-1} for MBAGD-A and MBAGD-H. The AcGGM content was significantly lower than the PAA content, and hence, the polysaccharide backbone related to the C—O—C stretching band was hardly detectable at 1072 cm^{-1} (MBAMP-A and MBAMP-H) and 1040 cm^{-1} (MBAGD-A and MBAGD-H).

Table III. Results of TG Analysis of AcGGM- and PAA-Based Hydrogels

	Dehydration ($T = 100°C$)	Main decomposition stage		
Sample	Weight loss %	T_{max} °C	Weight loss %	Residual weight at 600°C %
MBA-A	1.3	290.5	68.2	21.3
MBAMP-0	0.5	285.6	76	18.5
MBAMP-A	0.1	280	70.7	23.3
MBAMP-H	1.2	282.8	74.9	13.7
MBAGD-0	0.2	300.4	77.4	17.7
MBAGD-A	0.1	300.4	70.6	23
MBAGD-H	0.5	271.7	65.8	21.3

T_{max} represents the temperature of the highest weight loss rate.

C—O—C splitting in this case was due to the presence of —C— atoms next to —O— that could not be excluded or controlled during synthesis.[34] In the same wavenumber range, tertiary amine C—N stretching bands were also observed. Methylene chains gave rise to C—H stretching bands in the 2970–2800 cm^{-1} region and to scissoring bands in the 1350–1480 cm^{-1} range. The broad band typical of —OH stretching at 3264 cm^{-1} stemming from the polyhydroxylated polysaccharide backbone was also clearly visible, overlapped with the amide N—H stretching band.

In contrast to what was observed in the case of PAA-MA-AcGGM and PAA-MA-hydrolysate hydrogels, the FTIR spectrum of MBA-A (Figure 3) displayed a very strong C—O stretching band at 1025 cm^{-1} stemming from the AcGGM component in addition to the diagnostic bands typical of MBA, which indicated a higher AcGGM content in this sample. The band at 809 cm^{-1} originated from AcGGM C—C stretching, whereas that at 882 cm^{-1} can be attributed to residual alkene deformation.

All hydrogels were thermally characterized by DSC and TG analyses. The DSC thermogram for the second heating cycle, following a cooling cycle carried out at the same rate, is reported in Figure 4. For comparison, the thermograms of the reference materials are also reported. The glass transition temperatures or melting phenomena could not be detected in any of the samples, in agreement with the behavior of both reference PAA hydrogels and AcGGM. Substantial thermal stability was observed over the temperature range investigated, with no dramatic decomposition events. The TGA results are shown in Table III; in addition, the TGA curves of the hydrogels are available in the supporting information (Supporting Information Figure S2). The hydrogels typically displayed weight loss events due to dehydration at 100°C and main thermal decomposition events in the 200–450°C range, with residual masses reaching as low as 13.7%. The introduction of AcGGM and MA into the hydrogel composition apparently increased the thermal stability of the materials with respect to the "homopolymeric" PAA hydrogels. In fact, in most cases, the weight loss events of the AcGGM- and hydrolysate-containing hydrogels were lower than those of MBAMP-0 and MBAGD-0. For MBA-A (Figure 5, bottom), the main degradation event occurred between 250°C and 450°C, with residual masses reaching as low as 21.3%. All samples were stable at temperatures up to 200°C.

Hydrogel Swelling

The swelling behavior of the synthesized hydrogels was evaluated in water and buffer solutions at pH 2 and 9 (Figure 5). Hydrogels based on AcGGM were more swellable in aqueous media hydrolysate-containing hydrogels. This behavior was expected and can be ascribed to the higher cross-link density in the former case as well as the more hydrophobic lignin portion residing in

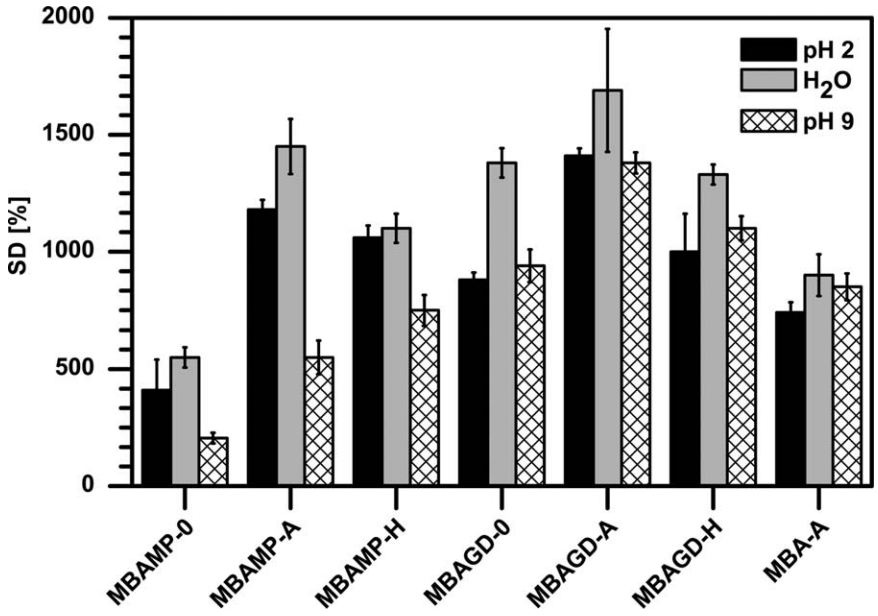

Figure 5. Degree of swelling (SD) in water and buffer media of PAA-based hydrogels.

Table IV. Shear Moduli for PAA-Based Hydrogels

Sample	G′ kPa	G″ kPa
MBA-A	7.1	0.6
MBAMP-0	24.0	0.3
MBAMP-A	4.0	0.2
MBAMP-H	10.8	3.7
MBAGD-0	0.7	0.02
MBAGD-A	0.2	0.006
MBAGD-H	3.9	0.2

the latter. Furthermore, all hydrogels containing MA and either AcGGM or hydrolysate swelled more than either the MBA-A or "homopolymeric" PAA hydrogels. The hydrophilic nature and carboxylated structures of the AcGGM and MA repeating units led to a greater driving force for water uptake. The MBAGD oligomer was synthesized from glycine and expected to be more hydrophilic than the MBAMP oligomer, which was reflected in the higher swelling capacity of the hydrogels cross-linked with MBAGD. All hydrogels showed greater swelling in water than in the buffer solutions, likely due to their higher ionic strength.

Figure 7. Color changes of heavy metal aqueous solutions of a) MBAGD-A and b) MBAMP-A upon hydrogel adsorption. From left to right: Native resins, Cu^{2+}, Ni^{2+}, and Co^{2+} solutions. [Color figure can be viewed in the online issue, which is available at wileyonlinelibrary.com.]

Rheological Behavior

In the water-swollen state, all hydrogel samples appeared as soft, transparent, and pliable materials that could be easily handled but did not withstand large stresses. The hydrogels were characterized by dynamic mechanical analysis in the shear stress mode over frequencies ranging from 0 to 100 rad/s and under an applied compressive force of 0.2 N. The trends of the storage and loss modulus versus frequency are reported in the supporting information (Supporting Information Figure S3), and the storage modulus (G') and loss modulus (G'') values are summarized in Table IV. All samples showed very low G' values, consistent with the low compressive force applied. In all cases, the storage modulus was higher than the loss modulus (G'') over the entire frequency range, indicating that the elastic response of the materials

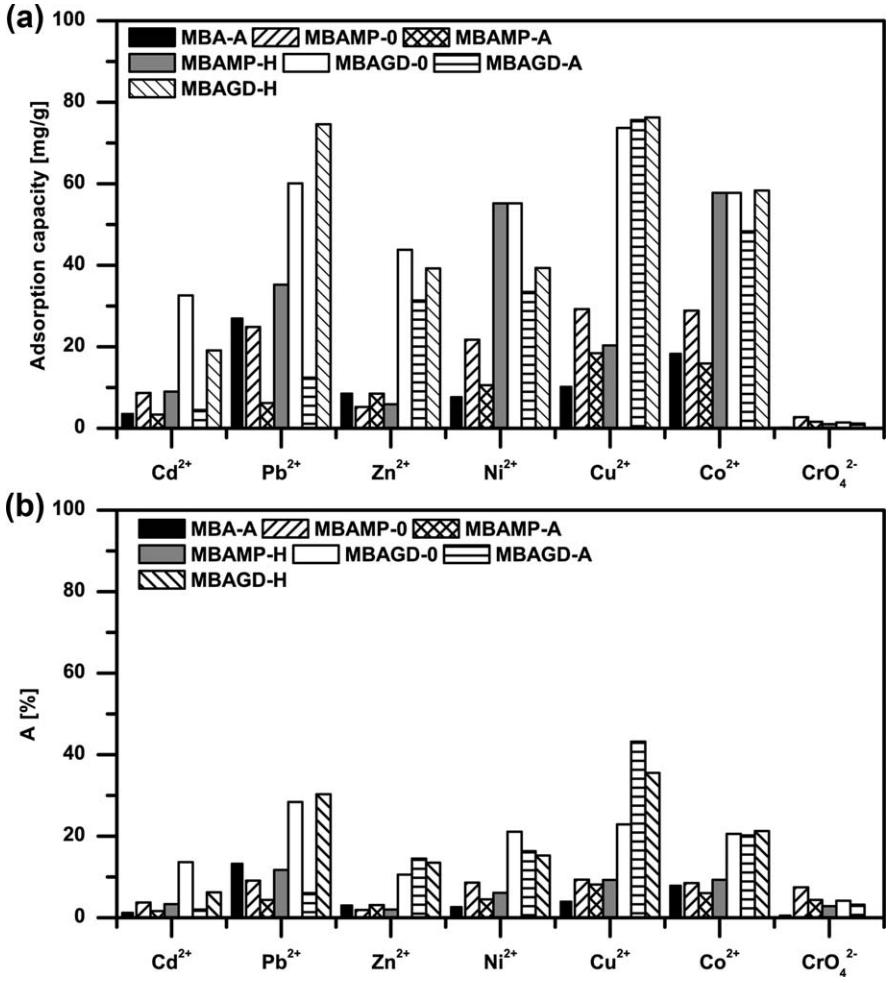

Figure 6. Absorption capacities (top) and metal abatement percentages (A %) (bottom) of PAA-based hydrogels in aqueous solutions with an initial metal ion concentration of 700 ppm.

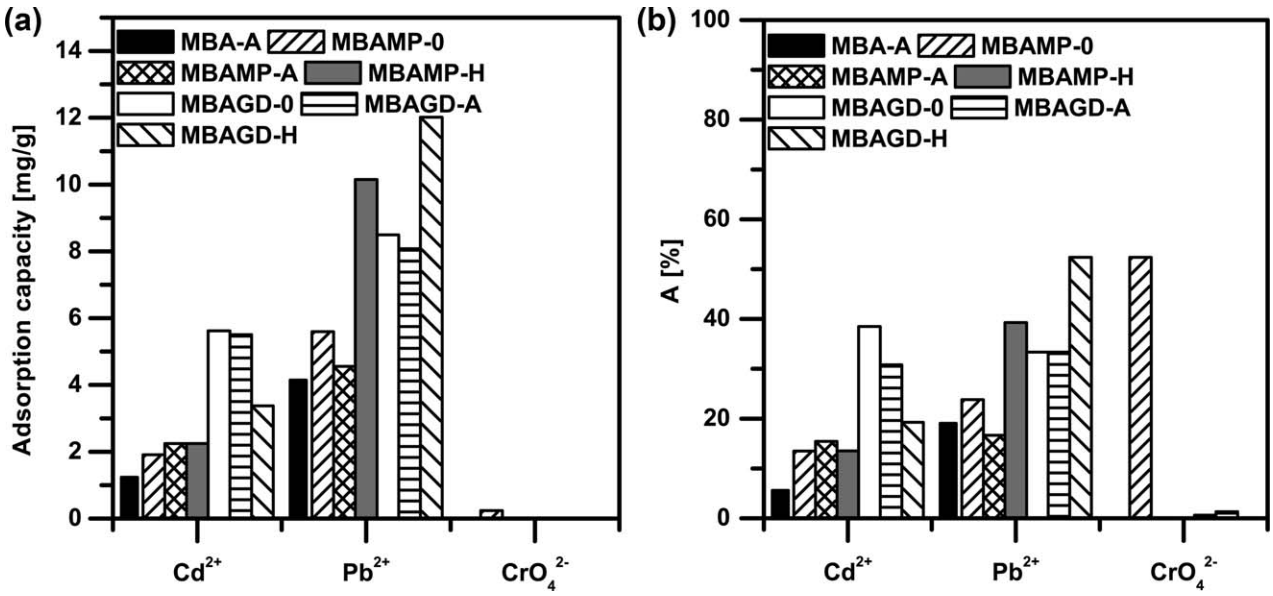

Figure 8. Absorption capacities (left) and metal abatement percentages (*A*%) (right) of PAA-based hydrogels in aqueous solutions with an initial metal ion concentration of 50 ppm for Cd^{2+} and Pb^{2+} and 4 ppm for CrO_4^{2-}.

prevailed over the viscous response and that the materials displayed solid-like behavior. Hydrogels cross-linked with MBAMP showed higher moduli than did the MBAGD-linked hydrogels, consistent with the higher hydrophilicity and swellability observed for the latter. The AcGGM hydrogels showed lower moduli than did the corresponding hydrolysate-based hydrogel, consistent with the fact that the former were more highly swollen.

Metal Ion Adsorption

Preliminary investigations of the heavy metal ion absorption capacity of the hydrogels were carried out in batch mode by incubating swollen hydrogel samples in separate heavy metal ion aqueous solutions until equilibrium concentrations were achieved. The initial and final ion concentrations of Cd^{2+}, Pb^{2+}, Zn^{2+}, Ni^{2+}, Cu^{2+}, and Co^{2+} were determined via complexometric titration with ethylenediamine tetraacetic acid (EDTA), whereas CrO_4^{2-} was determined by UV-vis spectrophotometry. A preliminary series of absorption tests was carried out in separate 700 ppm metal aqueous solutions to determine the hydrogel absorption capacity (Figure 6). The abatement percentage was calculated as follows:

$$A[\%] = \frac{\text{Absorbed}Me^{+}[\text{mg}]}{\text{Initial}Me^{+}[\text{mg}]} \times 100$$

Several relevant correlations between the observed capacities and the peculiar structural features of hydrogels were identified. The ion absorption capacities varied dramatically by varying the amine composition and were mainly driven by the PAA content. In particular, hydrogels cross-linked with MBADG and thus containing glycine structural units exhibited a higher Me^{2+} complexing ability than did the other hydrogels, suggesting a cooperative effect between the amine and carboxyl functionalities in ion complexation (Figure 6). For the same reason, the "homopolymeric" PAA hydrogels showed lower complexing abilities than those containing AcGGM or hydrolysate due to the higher $-COO^-$ content in the hemicellulose-containing networks. In general, the order of adsorption affinity towards Me^{2+} was $Cu^{2+}>Co^{2+}>Zn^{2+}\approx Ni^{2+}>Pb^{2+}>Cd^{2+}$, in relatively good agreement with the stability constants for amine complexes.[35] The same order of adsorption affinities ($Zn^{2+}>Pb^{2+}>Cd^{2+}$) was shown by another polysaccharide hydrogel, an amino-functionalized dextran hydrogel, at neutral pH. The adsorption of Zn^{2+} was in this case particularly high (500 mg/g) while the Cd^{2+} adsorption was very low (<3 mg/g).[5] A higher adsorption of Cu^{2+} compared with Pb^{2+} was in agreement with the behavior of a hemicellulose hydrogel based on arabinoxylan and cross-linked with acrylic acid.[17] The adsorption capacity of the arabinoxylan hydrogels was generally higher than those of the MBAGD- and MBAMP-based hydrogels and could be controlled by varying the ratio of acrylic acid showing the important contribution of carboxyl functionalities to the hydrogel behavior.[16,17]

The hydrogels were also assessed with respect to their complexation capacity towards the negatively charged noxious pollutant CrO_4^{2-}. In this case, the $-COO^-$ groups in MA repeating units and AcGGM did not significantly contribute to the absorption of the negatively charged ions. Hence, CrO_4^{2-} was adsorbed to a greater extent by the "homopolymeric" PAA hydrogel based on MBAMP, a model cationic PAA, than by the other hydrogels. The CrO_4^{2-} abatement percentages of the MBAMP cross-linked gels were higher than those of the gels cross-linked with MBAGD.

In some cases, particularly with respect Cu^{2+}, Ni^{2+}, and Co^{2+}, the sorption process resulted in intense and fast coloring (blue, green, and pink, respectively). This feature (Figure 7) may be in principle exploited in diagnostic kits or adopted as an indicator of the degree of exhaustion and, therefore, of the regeneration timing if the hydrogels are used for water purification.

In the case of Cd^{2+}, Pb^{2+}, and CrO_4^{2-}, the performance of all hydrogels was investigated in the low-concentration range as well to identify their potential for ion abatement in dilute solutions.

Adsorption from individual metal solutions containing 50 ppm Cd^{2+} or Pb^{2+} or 4 ppm CrO_4^{2-} demonstrated that the hydrogel complexing ability strongly depended on the metal ion concentration because the percent absorption decreased without following a regular trend (Figure 8). The abatement of Cd^{2+} varied between 12 to 38.5%, whereas the Pb^{2+} abatement ranged from 16 to 52%. Hydrogels cross-linked with MBAGD, containing dissociated glycine in the polymer chain, were consistently more efficient, whereas the MBA-A hydrogel showed lower abatements. The absorption capacities obtained were in some cases quite competitive with those of other materials reported in the literature.[36–39] In the case of CrO_4^{2-}, the abatement percentages were significant for MBAMP-0 (52.4%) and lower for MBAGD-0 (0.64%) and MBAGD-A (1.33%), while the remaining products showed no absorption towards CrO_4^{2-} in such diluted solutions.

CONCLUSIONS

Hemicellulose-based hydrogels were developed for heavy metal ions absorption and shown to be viable both when obtained from the highly purified softwood hemicellulose *O*-acetyl-galactoglucomannan (AcGGM) or a less refined biomass, a lignin-containing spruce hydrolysate. The hydrogels were prepared in aqueous solution by redox-initiated radical graft polymerization of methacrylic acid (MA) onto the AcGGM backbone in the presence of acrylamide end-capped poly(amidoamine) (PAA) oligomers as cross-linkers. Elemental analysis, FTIR, and rheology verified that cross-linked products with high mechanical integrity were successfully obtained. The PAA-MA-AcGGM hydrogels showed a higher degree of swelling in aqueous media as well as lower G' moduli than did the PAA-MA-hydrolysate gels, likely due to the lower cross-linking degrees of the former.

All hydrogels efficiently removed Cd^{2+}, Pb^{2+}, Zn^{2+}, Ni^{2+}, Cu^{2+}, and Co^{2+} from aqueous solutions, with absorption capacities of up to 76.3 mg/g. Furthermore, the hydrogels proved able to completely adsorb Cd^{2+} and Pb^{2+} from more diluted (50 ppm) solutions. In most cases, the absorption performances of the hydrogels improved with increasing PAA and carboxyl group concentrations, albeit without following a regular trend, indicating that the absorption was significantly driven by PAAs. The same trend was observed for the removal of Cr^{6+} as CrO_4^{2-}. Moreover, the absorption of several metal ions imparted intense coloring to the resins, a feature exploitable for analytical purposes such as the real-time detection of ions. All hydrogels were obtained at moderate cost by eco-friendly procedures according to a synthetic process characterized by potential scalability and environmental sustainability and by employing a renewable resource as the matrix material.

ACKNOWLEDGMENTS

The University of Milan and the Swedish research council FORMAS (project nr. 2011-1542) are thanked for their financial support.

REFERENCES

1. Marcovecchio, J. E.; Botte, S. E.; Freije, R. H. In Handbook of Water Analysis, 2nd ed.; Nollet, L. M., Ed.; CRC Press: London, **2007**, p 275.
2. Phillips, G. R.; Russo, R. C. Metal bioaccumulation in fishes and aquatic invertebrates. EPA-600/3-78-103. Duluth, Minn.: Environmental Protection Agency, **1978**.
3. Guilherme, M. R.; Reis, A. V.; Paulino, A. T.; Moia, T. A.; Mattoso, L. H. C.; Tambourgi, E. B. *J. Appl. Polym. Sci.* **2010**, *117*, 3146.
4. Zhao, L.; Mitomo, H. *J. Appl. Polym. Sci.* **2008**, *110*, 1388.
5. Demirbilek, C.; Özdemir Dinc, C. *Carbohydr. Polym.* **2012**, *90*, 1159.
6. Pourjavadi, A.; Doulabi, M.; Alamolhoda, A. A.; Tavakkoli, E.; Amirshekari, S. *J. Appl. Polym. Sci.* **2013**, *130*, 3001.
7. Hartman, J.; Albertsson, A.-C.; Sjöberg, J. *Biomacromolecules* **2006**, *7*, 1983.
8. Ryberg, Y. Z.; Edlund, U.; Albertsson, A.-C. *Biomacromolecules* **2011**, *12*, 1355.
9. Hansen, N. M. L.; Plackett, D. *Biomacromolecules* **2008**, *9*, 1493.
10. Nigam, J. J. *Biotechnol.* **2002**, *97*, 107.
11. Saha, B. C. *J. Ind. Microbiol. Biot.* **2003**, *30*, 279.
12. Söderqvist Lindblad, M.; Ranucci, E.; Albertsson, A.-C. *Macromol. Rapid Commun.* **2001**, *22*, 962.
13. Voepel, J; Edlund, U.; Albertsson, A.-C. *J. Polym. Sci. A Polym. Chem.* **2009**, *47*, 3595.
14. Yang, J.; Zhou, X. S.; Fang, J. *Carbohydr. Polym.* **2011**, *86*, 1113.
15. Sun, X. F.; Wang, H.; Jing, Z.; Mohanathas, R. *Carbohyd. Polym.* **2013**, *92*, 1357.
16. Peng, X.-W.; Zhong, L.-X.; Ren, J.-L.; Sun, R.-C. *J. Agr. Food Chem.* **2012**, *60*, 3909.
17. Zhong, L.; Peng, X.; Song, L.; Yang, D.; Cao, X.; Sun, R. *Separation Sci. Technol.* **2013**, *48*, 2659.
18. Dax, D.; Soledad Chavez, M.; Xu, C.; Willför, S.; Tiexeira Mendonca, R.; Sanchez, J. *Carbohydr. Polym.* **2014**, *111*, 797.
19. Maleki, L.; Edlund, U.; Albertsson, A.-C. *Carbohydr. Polym.* **2014**, *108*, 281.
20. Edlund, U.; Albertsson, A.-C. *J. Polym. Sci. A Polym. Chem.* **2012**, *50*, 2650.
21. Ferruti, P. *J. Polym. Sci. A Polym. Chem.* **2013**, *51*, 2319.
22. Ferruti, P.; Ranucci, E.; Bianchi, S.; Falciola, L.; Mussini, P. R.; Rossi, M. *J. Polym. Sci. A Polym. Chem.* **2006**, *44*, 2316.
23. Ferruti, P.; Ranucci, E.; Manfredi, A.; Mauro, N.; Ferrari, E.; Bruni, R.; Colombo, F.; Mussini, P.; Rossi, M. *J. Polym. Sci. A Polym. Chem.* **2012**, *50*, 5000.
24. Manfredi, A.; Ranucci, E.; Morandi, S.; Mussini, P. R.; Ferruti, P. *J. Polym. Sci. A Polym. Chem.* **2013**, *51*, 769.
25. Dahlman, O.; Jacobs, A.; Liljenberg, A.; Olsson, A. I. *J. Chromatogr.* **2000**, *891*, 157.
26. Jacobs, A.; Dahlman, O. *Biomacromolecules* **2001**, *2*, 894.
27. Saadatmand, S.; Edlund, U.; Albertsson, A.-C.; Danielsson, S.; Dahlman, O. *Environ. Sci. Technol.* **2012**, *46*, 8389.
28. Skoog, D. A.; West, D. M. In Fundamentals of Analytical Chemistry, 3rd Ed.; Holt-Saunders International Edition:, **1976**, p 272.

29. Knipe, J. M.; Chen, F.; Peppas, N. A. *J. Appl. Polym. Sci.* **2014**, *131*, DOI: 10.1002/APP40098.

30. Sandu, T.; Sarbu, A.; Constantin, F.; Vulpe, S.; Iovu, H. *J. Appl. Polym. Sci.* **2013**, *127*, 4061.

31. Panic, V. V.; Madzarevic, Z. P.; Volkov-Husovic, T.; Velickovic, S. J. *Chem. Eng. J.* **2013**, *217*, 192.

32. Milosavljević, N. B.; Ristić, M. Đ.; Perić-Grujić, A. A.; Filipović, J. M.; Štrbac, S. B.; Rakočević, Z. L.; Kalagasidis Krušić, M. T. *Colloid. Surface A* **2011**, *388* 59.

33. Peng, X.-W.; Ren, J.-L.; Zhong, L.-X.; Peng, F.; Sun, R.-C. *J. Agr. Food Chem.* **2011**, *59*, 8208.

34. Silverstein, R.; Webster, F.; Kiemle, D. J. In Spectroscopic Identification of Organic Compounds, 7th Ed; Wiley: **2005**; Chapter *2*, p 91.

35. Stability constants for Metal-ion complexes. In: Special Publications No. 17; Sillén, L. G., Martell, A. E., Eds; The Chemical Society: London, **1964**.

36. Yadanaparthi, S. K. R.; Graybill, D.; von Wandruszka, R. *J. Hazard. Mater.* **2009**, *171*, 1.

37. Fu, F.; Wang, Q. *J. Environ. Manage.* **2011**, *92*, 407.

38. Bhattacharyya, K. G.; Gupta, S. S. *Adv. Colloid Interfac.* **2008**, *140*, 114.

39. Babel, S.; Kurniawan, T. A. *J. Hazard. Mater.* **2003**, *B97*, 219.